J Solid State Electrochem (2010) 14:1377–1382
DOI 10.1007/s10008-009-0959-2

ORIGINAL PAPER

Initial stage of pore formation process in anodic aluminum oxide template

Na Wang · Wendi Zhang · Jipeng Xu · Bin Ma · Zongzhi Zhang · Qingyuan Jin · Eerke Bunte · Jürgen Hüpkes · Hans P. Bochem

Received: 31 July 2009 / Revised: 23 September 2009 / Accepted: 9 October 2009 / Published online: 10 November 2009

Abstract The initial stage of pore formation and the growth process in anodic aluminum oxide (AAO) template have been carefully investigated. Detailed features are found concerning the nanostructure configuration formed on the electropolished aluminum foil and the additional fine structures in the first and second anodization resulting from the current limitation effect during the beginning time of about 2 s. It sheds new light onto the mechanism of the pore-organizing process of AAO templates.

Keywords Anodic aluminum oxide film · Surface morphology · Pore-organization process · Scanning electron microscopy

Introduction

Porous anodic aluminum oxide (AAO) films have received increasing interest because of their potential applications in data storage, sensing, optoelectronics and photonics, etc. [1–4]. Researchers have successfully improved the fabrication technique of AAO template. Highly ordered self-organizing structures are achievable in a broader regime, and novel three-dimensional porous architectures are realized by pulse anodization of aluminum [5–7]. Besides, people also have been concentrating on the study of AAO growth mechanism. Several models have been proposed to explain the self-organized porous structure within AAO. It is generally accepted that mechanical stress resulting from the volume expansion during oxidation promotes the formation of ordered hexagonal pore arrays. The growth of porous alumina contributes to the equilibrium of oxide growth at the metal-oxide interface and field-enhanced dissolution at the oxide–electrolyte interface [8, 9]. Nonetheless, we still need more experimental proofs for these models.

We can expect naturally that the detailed study of the initial stages of the pore growth is very essential to understand the AAO growth mechanism. Theoretical consideration of this process indicates that pore formation is initiated by the activation energies of the interfacial reaction and the elastic stress caused by the volume expansion [10, 11]. From the very beginning of the pore formation, i.e., the electropolishing process before anodization, extensive studies have also been conducted by electropolishing pure polycrystalline aluminum foil at various voltages and durations. Ordered topographies with hexagonal symmetry were reported at cell voltage E=30–50 V [12–14].

In this work, we report the existence of nanostructure patterns with shallow pits on the surface of aluminum foils electropolished at 20 V for 15 min. The dependence of the topography properties on the anodization time has been investigated to gain more insights into the incipient pore-organizing process of the AAO template. In addition, the

N. Wang · J. Xu · B. Ma · Z. Zhang · Q. Jin (✉)
Laboratory of Advanced Materials, and Department of Optical Science and Engineering, Fudan University,
Shanghai 200433, China
e-mail: qyjin@fudan.edu.cn

W. Zhang · E. Bunte · J. Hüpkes
IEF5-Photovoltaik,
Forschungszentrum Jülich GmbH,
52425 Jülich, Germany

H. P. Bochem
Institut für Bio- und Nanosysteme (IBN-PT),
Forschungszentrum Jülich GmbH,
52425 Jülich, Germany

effect of the limited current signal on the initial pore structure is investigated, which is due to the overflowed power supply (setting at the constant-voltage mode) in the first few seconds of the anodization process. This is expected to help us understand the formation mechanism of AAO template and to control better the fabrication technique.

Experimental details

The experiments were carried out in a home-built glass cell. A platinum disk worked as a cathode and the aluminum foil as an anode. The distance between the cathode and anode was maintained at 4.1 cm, and the area of aluminum foil exposed to the electrolyte was 2.5 cm^2.

High purity aluminum foils (99.99%) were preannealed at 500 °C for 5 h under forming gases (95% N_2+5% H_2) to obtain homogeneous conditions for pore growth over large areas. The foil was etched in 0.2 M NaOH aqueous solution until bubbles occurred over the surface and then ultrasonically cleaned with deionized water. After degreasing by ethanol, it was electropolished in a mixture of $HClO_4$ and C_2H_5OH (1:10 by volume) under a constant voltage to lower the roughness of the aluminum surface. Anodization was carried out in 0.3 M aqueous oxalic acid at 40 V and 5 °C for varying lengths of time ranging from 1 to 600 s [9]. Before the study of the initial pore-organizing process in the second anodization, a 1 h anodization was conducted, and the formed alumina film was stripped away by immersing the foil in a mixture solution of H_3PO_4 (6 wt %) and H_2CrO_4 (1.8 wt%) at 60 °C for 30 min.

All voltages and currents were produced and recorded by a PC-controlled SourceMeter 2400 (Keithley Instruments, Inc.) system. The responded current–time curves were used to monitor the anodization process as well as to analyze the growth mechanism. Field-emission scanning electron microscopy (FE-SEM) measurements were performed by a Leo Gemini FE-SEM working at 20 kV.

Results and discussion

Aluminum foils with mirror-like surface are obtained after being electropolished under 20 V for 15 min. The morphology of this smooth exterior is detected by FE-SEM with high resolution and is shown in Fig. 1 (50 and 400 K times magnification for (a) and (b), respectively). From the top view of the electropolished film (see Fig. 1(a)) where the brightness of spots reflects fluctuation on the surface, we find that the nanopattern structure exists on the whole aluminum foil. Some pinholes are also observed on the surface, which could be points where dislocations

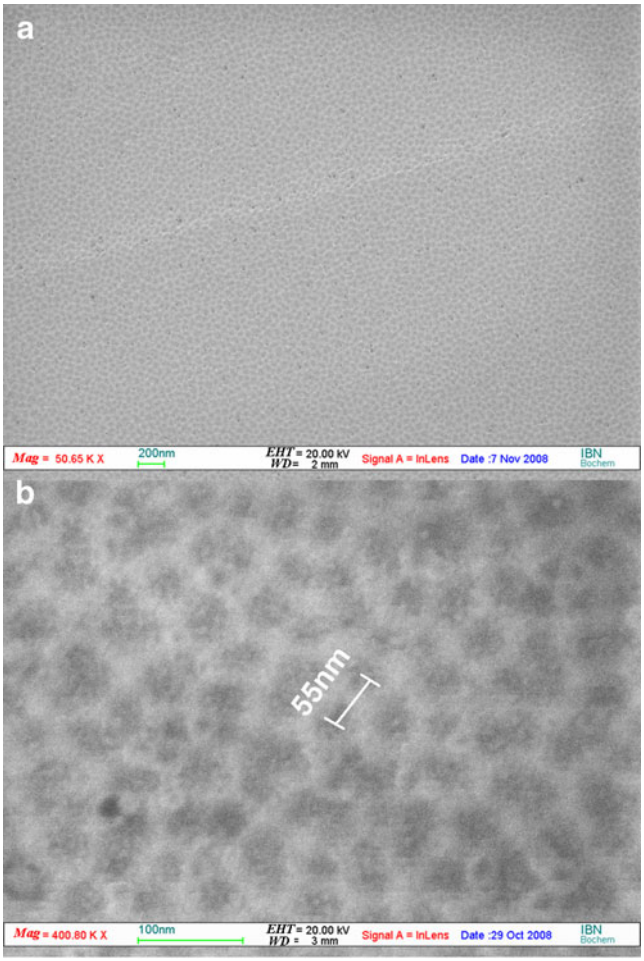

Fig. 1 **a** 50 K × and **b** 400 K × times enlarged FE-SEM images of the aluminum surface electropolished at 20 V for 15 min

emerge. Enlarged scale in Fig. 1(b) lets us see clearly that there is an arranged porous structure on the surface with disordered quasicircular pore shapes and a large size distribution. The typical interpore distance (D_{int}) is about 55 nm. The reason of irregular holes is supposed to be that the fusion occurred among two or three circular holes. Some controllable nanostructures with relatively straight channels and small D_{int} have been achieved via improving the pretreatment of electropolishing. A more detailed analysis of its influence on the structural properties of AAO template will be reported in our next paper. Detailed experimental observation is required for the further understanding of the pore-organizing process in the electropolishing treatment as well as the anodization process.

A standard two-step anodization process is performed to fabricate the AAO template. The anode current, as a function of the anodization time, is plotted in Fig. 2(a) and (b) for the first and second anodization, respectively. Typically for both cases, the current starts with a high value due to the clean aluminum surface, decreases quickly to a nadir along with the formation of nonconductive alumina,

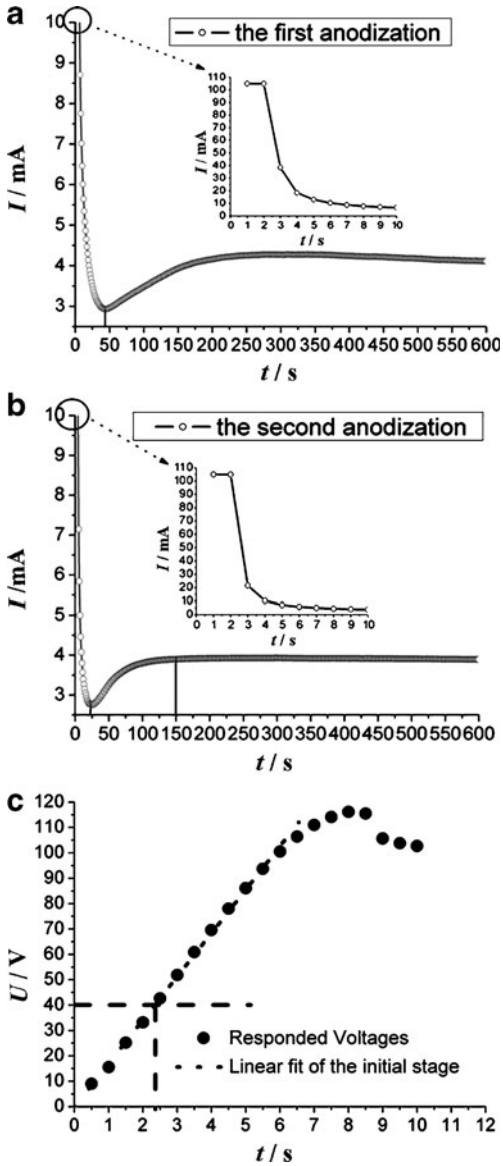

Fig. 2 The anode current as a function of time in the **a** first and **b** second anodization, **c** responded voltages, and the linear fitting setting the power as a constant current supply at 105.5 mA

and then, increases to the stable value indicating the finish of pore-organizing process. The time when the current reaches its lowest point is about 43 and 24 s and around 10 min and 150 s, respectively, for the current to become a constant value after anodizing. This indicates that pore-organizing process is much faster in the second anodization since the pore structures organized in an ordered way under the guiding effect of hexagonal concave patterns formed in the first one. Besides the above normal behavior for current evolution curves, we find that the recorded current maintains at the value of 105.5 mA during the first 2 s though we have set the power in a constant-voltage mode at 40 V. This is because the SourceMeter 2400 has a full-scale reading of 105.5 mA for the current measurement at 200 V V-source range. The power supply actually provides a limited current signal of 105.5 mA rather than a constant voltage at 40 V in the initial 2 s. By setting the electric source as a constant current supply at 105.5 mA, we obtain that the feedback voltage has a linear relation with time until 5.5 s from 0 to 95 V, as shown in Fig. 2(c). Thus, the aluminum foil is actually anodized at a linearly increased potential (constant current) for 2.3 s and then at a fixed voltage of 40 V. The working state of SourceMeter 2400 is also confirmed on its panel display.

In order to study the pore-organizing process especially the initial pore formation within 2.3 s before the voltage reaches 40 V and its effect on the succeeding process, we fabricate a series of samples with varying length of anodization time ranging from 1 s to 10 min that covers the main formation stages of the AAO template. Figure 3(a) to (e) shows the surface topography of aluminum foils anodizing at 40 V for various time in the first anodization. White spots are observed on the surface of samples anodized for 1 and 5 s (Fig. 3(a) and (b)) that probably originated from the anodization in a fixed current mode from the beginning. This is confirmed by the surface of the sample anodized at a small voltage of 5 V for 5 s (no power limitation when the 20 V V-source range is selected), where white spots are much clearly observed as shown in Fig. 3 (f). As we know from the linear dependence of D_{int} on the anodization voltage [9], D_{int} of AAO template anodizing at 40 V should be about 110 nm. But we obtained a nanopattern structure with much smaller value of D_{int} (typically around 50–60 nm). This attributes to the anodization under small voltages coming from power limitation and the guiding of electropolished surface. Comparing Fig. 3 with Fig. 1, we find that the pore-organizing process starts immediately after switching on the bias and tends to form the structure based on the nano-pattern remaining on the surface of the electropolished aluminum foil. After several seconds (larger than 2.3 s), final voltage of 40 V is reached. The constant current anodization process is replaced by the constant voltage. White spots disappear after anodizing for 300 s, and D_{int} is found to increase through a way that some pores stop growing along with the anodization time (as indicated by circles in Fig. 3(d) and (e)). The pore formation process enters an equilibrium stage after anodizing for about 10 min (deduced from the curve of Fig. 2(a), and its morphology is shown in Fig. 3(e)).

After removal of the alumina layer, the patterned aluminum foil is used for the second anodization. Figure 4 (a) and (b) shows the morphology of the patterned substrate viewed from the top and at an angle of 60 degree, respectively. Ordered hexagonal structure with concave patterns and D_{int} of about 110 nm are observed on the

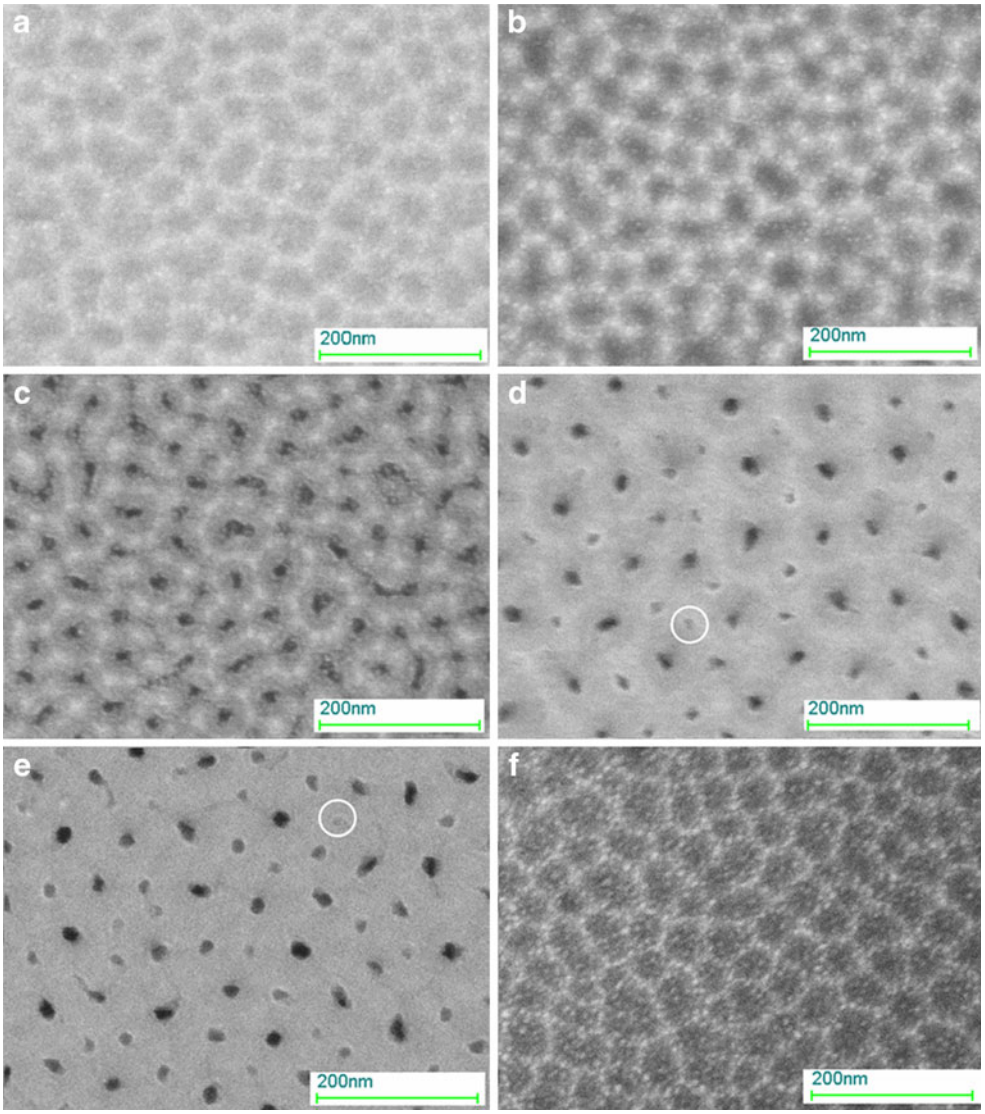

Fig. 3 The FE-SEM image of AAO films formed in the first anodization, which are obtained under anodizing potential of 40 V for **a** 1, **b** 5, **c** 40, **d** 300, and **e** 600 s and of 5 V for **f** 5 s on the electropolished aluminum surface

surface. This self-organized periodic structure serves as a mask for the following anodization.

Figure 5(a) shows the exterior topography of AAO template anodized at 40 V for 30 s in the second anodization. Same as what we have mentioned in the first anodization, the second anodization within the initial several seconds performs at a fixed current signal before reaching the setting voltage of 40 V. Previous studies have proved that porous structures are developed even under ultra-low anodic potentials [15]. According to our anterior

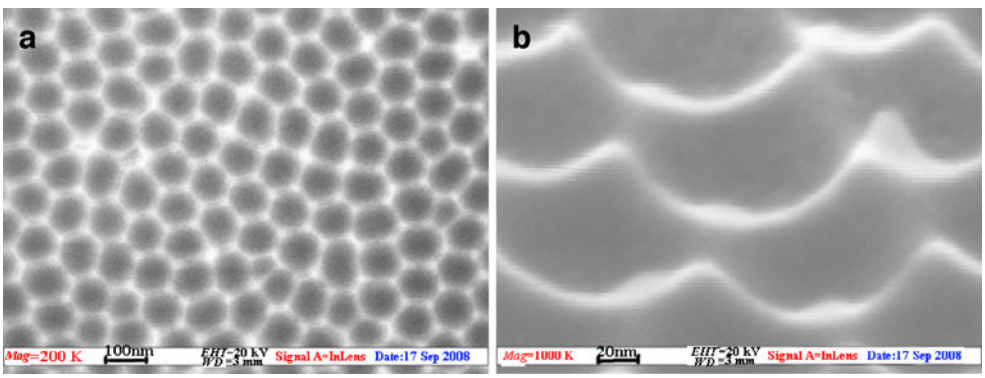

Fig. 4 FE-SEM images of the aluminum substrate used for the second anodization, which are observed at an angle of **a** 90 and **b** 60 degrees

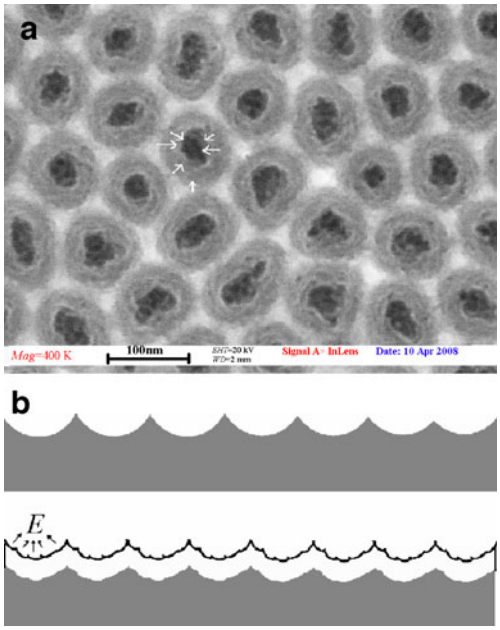

Fig. 5 **a** The top view FE-SEM image of the AAO film anodized for 30 s in the second anodization. **b** A schematic diagram of the initial pore-organizing process under the guiding of concave patterns

results, pore-organizing process is an immediate action after switching on the bias. It is reasonable that the oxidation at a current-limited signal leads to instabilities, which develop into nanopatterns with smaller D_{int} under the effect of field-enhanced dissolution. Then, what we would expect at the beginning of the second anodization is the formation of small shallow patterns along the electric field direction superimposing on the hexagonal concaved template [16], as schematically depicted in Fig. 5(b). Along with the anodization, the central part of each concave dissolves preferentially to form the initial pore, which is attributed to the larger current flow distribution at this position (more apparently with the increase of anodizing time). The FE-SEM image in Fig. 5(a) presents this superimposition results that some steps exists in the inner of pores (indicated by arrows).

Morphology changes over the processing time in the second anodization are disclosed in Fig. 6. All the images are recorded under the same magnification condition so that the size of topography can be directly compared. White spots are clearly observed on the surface of samples anodized for 10 and 25 s and then gradually vanished under the field-enhanced dissolution. This observation is consistent with the trace study of AAO template that the initially formed oxide locates on the film surface [17]. No step-inside-pore feature exhibits on the surface of sample anodized for 10 s, which attributes to the fact that the growth process plays a dominant role at this stage. With increasing effect of dissolution, the fine step structure appears and becomes very distinct. Although the recorded current maintains at a constant value after anodizing for 150 s (shown in Fig. 2(b)), changes of the surface morphology continue. Concave masks as well as steps

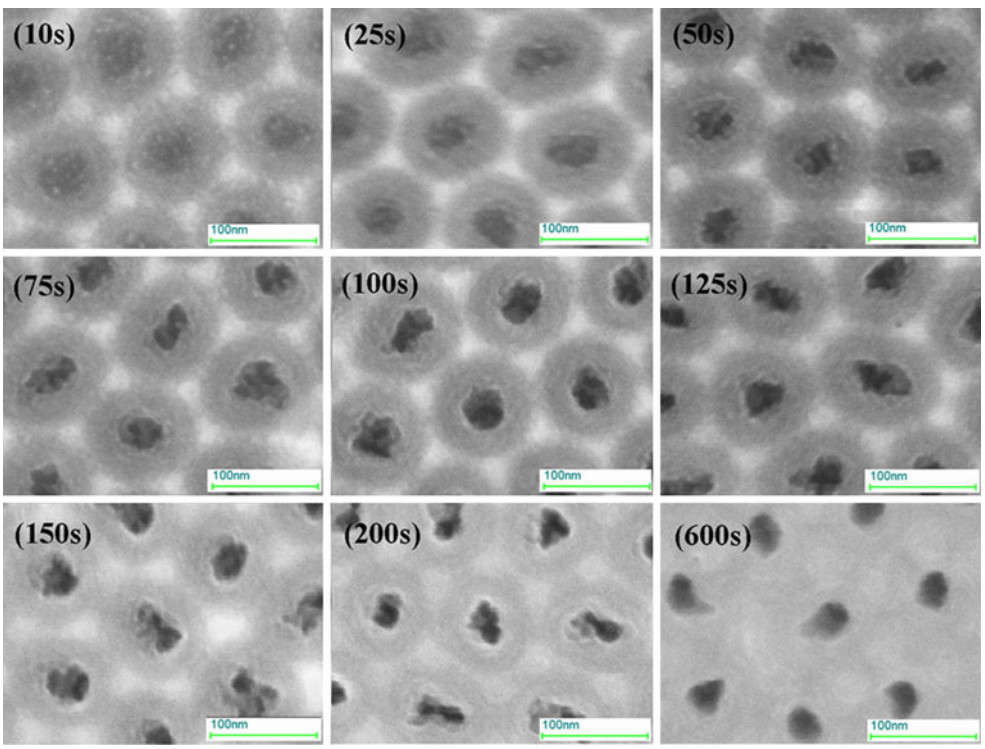

Fig. 6 The FE-SEM image of AAO films anodizing at 40 V for 10 to 600 s in the second anodization

inside pores, gradually disappear after 10-minute's anodization, which signify the accomplishment of pore-organizing process.

Conclusions

The pore-organizing process of AAO template, especially at the beginning stage of anodization, is discussed in detail. Pore formation begins immediately after switching on the anodic bias and is incipiently guided by the nano-patterned fluctuation originated from the electropolishing treatment of the aluminum foil. An unexpected current-limited signal from power limitation within the first 2.3 s is discovered to master the initial stage of anodization. Nanopatterns with a smaller D_{int} in the first anodization and the additional fine step structure in the second anodization are observed. The feature that the AAO template growth is quite sensitive to the disturbance at small anodizing potential makes the above results possibly useful in fabrication of ordered AAO templates with ultrahigh density for some small devices.

Acknowledgments This work is supported by the NSF of China (grant numbers 50771032, 50771033, 10604016, and 60678008) and the National Basic Research Program of China (2009CB929201).

References

1. Nielsch K, Müller F, Li AP, Gösele U (2000) Adv Mater 12:582–586
2. Hahm J, Lieber CM (2004) Nano Lett 4:51–54
3. Gudiksen MS, Lauhon LJ, Wang JF, Smith DC, Lieber CM (2002) Nature 415:617–620
4. Li AP, Müller F, Birner A, Nielsch K, Gösele U (1999) Adv Mater 11:483–487
5. Masuda H, Fukuda K (1995) Science 268:1466–1468
6. Lee W, Ji R, Gösele U, Nielsch K (2006) Nat Matters 5:741–747
7. Lee W, Schwirn K, Steinhart M, Pippel E, Scholz R, Gösele U (2008) Nat Nanotechnol 3:234–239
8. Jessensky O, Müller F, Gösele U (1998) Appl Phys Lett 72:1173–1175
9. Li AP, Müller F, Birner A, Nielsch K, Gösele U (1998) J Appl Phys 84:6023–6026
10. Singh GK, Golovin AA, Aranson IS (2006) Phys Rev B 73:205422
11. Sample C, Golovin AA (2006) Phys Rev E 74:041606
12. Bandyopadhyay S, Miller AE, Chang HC, Banerjee G, Yuzhakov V, Yue DF, Ricker RE, Jones S, Eastman JA, Baugher E, Chandrasekhar M (1996) Nanotechnology 7:360
13. Ricker RE, Miller AE, Yue DF, Banerjee G, Bandyopadhyay S (1996) J Electron Mater 25:1585
14. Guo WD, Johnson DT (2004) J Cryst Growth 268:258
15. Zhang F, Liu XH, Pan CF, Zhu J (2007) Nanotechnology 18:345302
16. Yin AJ, Guico RS, Xu J (2007) Nanotechnol 18:035304
17. Skeldon P, Thompson GE, Garcia SJ, Iglesias L, Blanco CE (2006) Electrochem Solid State Lett 9:B47–B51